Molecular cluster studies of binary alloys: LiAl†

D. E. Ellis, G. A. Benesh, and E. Byrom*
Department of Physics and Astronomy and Materials Research Center, Northwestern University, Evanston, Illinois 60201
(Received 6 June 1977)

The electronic structure of the ordered Zintl ($B32$) phase of LiAl has been studied in a molecular-cluster model within the framework of the Hartree-Fock-Slater theory. Li_5Al_4 and Al_5Li_4 clusters were embedded in a potential field representative of the alloy environment; energy levels and wave functions were obtained by self-consistent iteration. Density-of-states and charge-density results are used to interpret NMR and electrical-conductivity studies. The case of a single Li vacancy was also treated, and discussed in the light of positron-annihilation data.

I. INTRODUCTION

LiAl is a type I-III compound which crystallizes in the Zintl phase, $B32$ structure, of which NaTl is the prototype. Lithium alloys are currently of interest because of their potential usefulness as anodic materials in high-energy density batteries. LiAl is a particularly good candidate because of its relative stability compared to lithium metal. Other $B32$-type Li alloys include compounds with group II elements such as LiCd and LiZn, as well as compounds with group III elements. The structure itself can be described as two interpenetrating diamond lattices, one formed from each constituent. Each atom then appears at the center of a cube formed by its eight nearest neighbors. The local site geometry is tetrahedral with four atoms of each type occupying the cube vertices as shown in Fig. 1.

Very little is known about the electronic structure of LiAl. In the original work of Zintl and Brauer,[1] it was proposed that the Li atom transferred an electron to the type IIIa atom in I-III compounds. This atom would then behave as a IVa atom (such as C or Si) in forming a diamond lattice, with the Li atoms forming a second, rather loosely bound diamond lattice. This hypothesis is at least consistent with several NMR results of Schone and Knight.[2] They observed that the lattice constant was determined by the radius of the III atom, the nearest-neighbor distance of LiAl being twice the Goldschmidt radius of pure Al. Secondly, they concluded that aluminum atoms never substitute for lithium in the lattice. From this result, they argued that a defect phase occurs in LiAl exhibiting a permanent concentration of vacancies on the Li sublattice. Thirdly, an activation energy of only 0.15 ± 0.02 eV was found for the Li atoms, indicating high ionic mobility. The NMR frequency shifts (Knight shifts) for several alloys were determined; for LiAl the ^{7}Li shift was less than 0.005% and the ^{27}Al shift was $< 0.01\%$, substantially smaller than the pure-metal shifts of 0.025% and 0.16%, respectively.

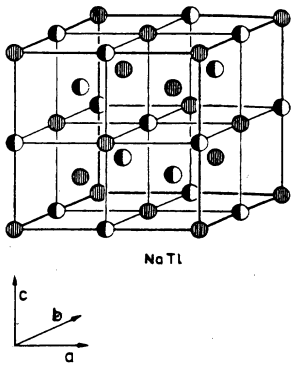

FIG. 1. Crystal structure of $B32$ (Zintl) compounds [W. B. Pearson, *The Crystal and Physics of Metals and Alloys* (Wiley-Interscience, New York, 1972)].

Bennett carried out NMR studies on a number of $B32$ alloys and proposed a band structure for LiAl with a filled "Li 2s" band lying well below the Fermi energy.[3] The higher bonding valence bands populated by the remaining Al 3s and 3p electrons would just be filled as in the diamond structure. This model predicts a charge transfer in precisely the *opposite* direction to that proposed by Zintl and Brauer. In the defect phase of LiAl, the top of the conduction bands would be slightly depopulated, leading to a "semimetal" (actually a defect-structure metal) in Bennett's model.

Recently, measurements of the ^{7}Li NMR relaxation rate T_1^{-1} were used to determine the degree of Li-ion motion and its dependence upon Li sublattice vacancy concentration.[4] Measurements of T_1^{-1} versus temperature for ^{27}Al were used to propose that the observed electric-field gradient is due to Li vacancies. An activation energy of 0.13 eV for Li diffusion was found, in agreement with the earlier work of Schone and Knight.

The molar magnetic susceptibilities of lithium alloys were measured by Yao[5] who found that the

conduction-electron susceptibility of LiAl was very small and positive, characteristic of a weak paramagnet.

Cristea *et al.* have measured the electrical resistivity of LiAl as a function of composition and temperature.[6] The resistivity of stoichiometric LiAl at 273 K was found to be 2×10^{-7} Ωm, with a linear increase of ρ with temperature over the interval 77 to 300 K. The resistivity was found to increase abruptly with increasing Li concentration over the 48–52 at.% interval studied. The resistivity results characteristic of a normal metal appear to contradict the semimetallic conjecture of Bennett. Preliminary calculations made by Switendick using the augmented-plane-wave (APW) energy-band method suggest a normal metal (but are also consistent with a semi-metal) with a low-lying s valence band.[7]

In the present molecular-cluster studies, we have found considerable charge transfer from the Li $2s$ state into a diffuse "Li $2p$" state, but with a very small charge transfer between atoms. The density of states at the Fermi energy $D(E_F)$ and Pauli paramagnetic spin susceptibility are estimated to be similar to Li metal. The conduction s-electron densitites at the Fermi energy, ρ(Li, E_F) and ρ(Al, E_F) are small compared to the metal, consistent with the Knight-shift data.

Our lowest band is indeed s-like, but primarily of Al-3s character. We suggest x-ray emission experiments (Li K, Al $L_{\mathrm{II,\,III}}$) to confirm or disprove this model.

II. THEORETICAL MODEL AND COMPUTATIONAL PROCEDURE

The Hartree-Fock-Slater one-electron model is well described in the literature,[8] and has been successfully applied to a variety of metallic systems using both periodic Bloch function representations and localized molecular cluster models.[9–11] The essential point of this theory is replacement of the nonlocal Hartree-Fock exchange operator by a local potential, derived from the theory of a free-electron gas,

$$V_x(\vec{r}) = -3C\left(\frac{3\rho(\vec{r})}{8\pi}\right)^{1/3}. \tag{1}$$

Here C is a constant (taken equal to $\frac{2}{3}$ in this work) and ρ is the electronic charge density. With the model Hamiltonian thus derived, one can proceed to set up self-consistent computational procedures for determining eigenstates ψ_n, energies ϵ_n, and the charge density.

A. Variational method

Molecular orbital energies and wavefunctions were obtained by a discrete-variational procedure described previously.[10,11] In the present work, numerical free-atom basis functions $\{A_j\}$ were used (which were calculated by solving the self-consistent free-atom problem), consisting of Li: 1s, 2s, 2p, and Al: 1s, 2s, 2p, 3s, 3p. Matrix elements of the Hamiltonian and unit (overlap) operators were obtained by direct numerical integration. A numerical precision of ~0.1 eV in valence level energies was obtained with 500 integration points. The matrix scalar equation $(H-ES)C=0$ was solved by standard procedures to obtain energies and the wavefunction expansion

$$\psi_n = \sum_{j=1}^{N} A_j(\vec{r})\,C_{jn}. \tag{2}$$

B. Self-consistent potential

We are motivated to construct a localized representation for electronic states of alloys, because of the great importance of localized defects, disorder, and impurities in these systems. One can expect that the external boundary conditions imposed on a cluster model will have highly significant effects because of the diffuse nature of metallic wavefunctions; thus point-charge or boundary-sphere approximations commonly used in cluster calculations on ionic and covalent solids[12–14] will be inadequate.

Fermi-Dirac statistics were invoked to determine occupation numbers f_i for molecular-orbital (MO) levels and the *cluster density* was constructed.

$$\rho_{\mathrm{cluster}} = \sum f_i\,|\psi_i(\vec{r})|^2. \tag{3a}$$

This was decomposed approximately by Mulliken populations,[15] as

$$\rho_{\mathrm{cluster}} \approx \rho_{\mathrm{SCC}} = \sum_{\nu nl} f^{\nu}_{nl}\,|R_{nl}(r_\nu)|^2, \tag{3b}$$

where f^{ν}_{nl} is the population for atom ν of the nl atomic shell.

The *crystal charge density* is then constructed for the next iteration cycle by extending the sum over atoms to infinity, and averaging results from previous cycles in the usual fashion, see Fig. 2(a). The resulting periodic self-consistent-charge density ρ_{SCC} is then completely analogous to that developed in our previous free-molecule and ionic cluster models.[11] The immediate use of the full periodic potential resulting from ρ_{SCC} in cluster calculations presents certain dangers for variational calculations, because of the deep potential wells localized on atoms which are near neighbors to the cluster. A sufficiently flexible basis set will attempt to describe "exterior core states" not associated with the cluster. The Pauli exclusion

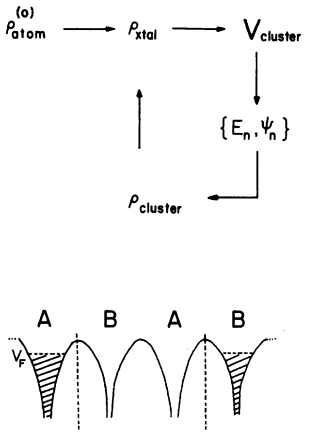

FIG. 2. (a) Schematic of self-consistency loop for cluster embedded in solid. (b) Schematic of truncated crystal potential used in calculating AB cluster levels embedded in the periodic solid.

principle, of course, acts to prevent transfer of electrons from the cluster into filled exterior states, and this constraint is most conveniently described in the pseudopotential formalism.[16] We have chosen to mimic the results which might be obtained by laborious pseudopotential calculations, by simply truncating exterior potential wells [Fig. 2(b)], thus introducing one empirical parameter in the present model. The sensitivity of our results to this well-depth parameter is slight, and will be discussed with the results.

C. Densities of states

The population contribution from atom νnl to the pth molecular orbital denoted by $f^{\nu}_{nl,p}$ is used in a definition of the local density of states (DOS)

$$D^{\nu}_{nl}(E) = \sum_{p} f^{\nu}_{nl,p} \frac{\sigma/\pi}{(E-\epsilon_p)^2+\sigma^2}. \quad (4)$$

This definition is chosen so that the discrete DOS is smoothed into a continuous distribution. The Lorentzian width parameter σ was chosen to be 1 eV, a value consistent with the uncertainties of our calculations and the small cluster size. The total density of states is then given by:

$$D(E) = \sum_{\nu nl} D^{\nu}_{nl} = \sum_{p} \frac{\sigma/\pi}{(E-\epsilon_p)^2+\sigma^2}. \quad (5)$$

The total DOS may be compared to photoemission spectra in a crude constant-matrix-elements approximation, in the occupied region $E \leq E_F$. The region $E > E_F$ is accessible by excitation techniques such as electron-energy-loss spectroscopy (EELS) as well as conventional optical methods. Although the cluster DOS is *not* an accurate representation of the complete energy band DOS of the periodic solid, we will find it useful to make comparisons between Li, Al, and LiAl cluster results in the vicinity of E_F. This approach leads to a certain cancellation of errors and permits a semiquantitative discussion of induced spin densities

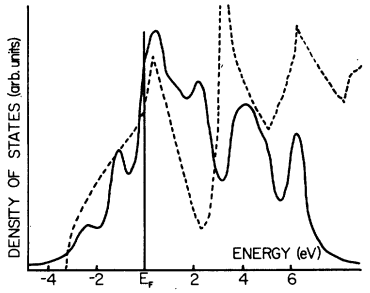

FIG. 3. Comparison of energy-band density of states (Ref. 17) (dashed line) and Li_9 cluster (solid line) density of states for lithium metal.

and NMR Knight shifts.

To gain an impression of the deviations between cluster densities of states and full band structure results, we performed calculations on Li_9 clusters representative of the bcc lithium metal structure. The self-consistent band structure data of Ching[17] are compared with the cluster DOS in Fig. 3, in which the two Fermi energies have been matched. The overall comparison is reasonably satisfactory and similar to that found for other metals.[18] The spurious peaks in the cluster DOS could be easily reduced by increasing the Lorentzian level width; however, this also has the effect of filling in genuine gaps observed in the band results, and in increasing the apparent conduction bandwidth.

The partial DOS analysis permits a discussion of x-ray emission spectra, where atomic dipole selection rules are approximately valid. Analysis of AlK, Al$L_{II,III}$ and LiK data would give an essentially complete characterization of composition of occupied conduction states.

III. RESULTS

A. Self-consistent potential

Two molecular clusters exhibiting the full T_d point group symmetry of the $B32$ structure were used in the LiAl calculations. Each cluster consisted of a central atom, either Li or Al, and its eight nearest neighbors. The cube edge was taken to be 6.01 a.u.[1]

As described above, the cluster potential was constructed from a simple self-consistent embedding model based upon the Mulliken population analysis of occupied molecular orbital levels. Inclusion of Coulomb and exchange interaction with the atoms external to the cluster proved to be essential in obtaining charge densities and densities of states which were relatively invariant to the cluster origin (Al_5Li_4 versus Li_5Al_4) and to the atom position (center versus periphery of cluster). In the absence of the crystal contributions to the potential, charge was observed to pile up in the in-

terior of the cluster, since peripheral atoms were unable to "see" the attractive bonding interactions with exterior atoms. Variation of properties with the pseudopotential parameter V_F used to truncate the potential wells of exterior atoms was found to be slight, the main effect being a uniform shift of the cluster Fermi energy. For these metallic systems, there is some virtue in choosing $V_F = E_F$, but values in the range 5–10 eV produce very acceptable results.

Charge transfer between unlike atoms (as defined by Mulliken populations) implies a buildup of charge on clusters used here. In earlier studies on ionic systems a simple renormalization of valence occupation numbers before projection onto the infinite crystal was found to be a satisfactory procedure[14] and was also used here. Since the calculated charge transfer is rather small, renormalization produces very minor effects.

B. Density of states

The total density of states for the Al-centered and Li-centered clusters are shown in Fig. 4. The two DOS curves are seen to be quite similar, with features insensitive to the cluster origin and crystal potential parameters. The Fermi energy lies on a sharply rising DOS peak, indicative of a normal metal. The prominent peak at ~6 eV below E_F is predominantly of Al3s character and the structure around E_F is dominated by Al3p character. Although understanding details of the DOS requires a band structure model, it is clear that the low-lying "Li 2s" band postulated by Bennett[3] would be better described as "Al 3s". Moreover, the MO eigenvectors display considerable Al s, p and Li s, p hybridization and mixing; partial densities of states are discussed further below in connection with predicted x-ray emission spectra.

C. Charge-density and Knight-shift estimates

The self-consistent charge density for the Li-centered cluster is plotted along three symmetry

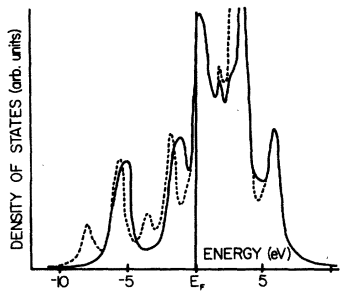

FIG. 4. Density of states for Li_5Al_4 (solid line) and Al_5Li_4 (dashed line) clusters determined in the self-consistent crystal field.

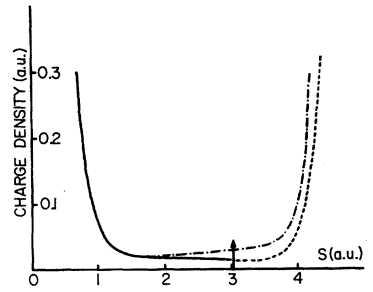

FIG. 5. Charge density of Li_5Al_4 cluster plotted along symmetry directions: [100], solid line; [111], dashed line; and [$\bar{1}\bar{1}\bar{1}$], broken line.

lines in Fig. 5. The density is quite spherical out to a distance of ~2 a.u. from the center of the cluster; beyond the midbond distance (indicated by a vertical arrow) the [111] density rises rapidly as the neighboring Li atom is approached, and still more rapidly in the [$\bar{1}\bar{1}\bar{1}$] direction toward a neighboring Al atom. Very little evidence is seen for the covalent bonding suggested by Schone and Knight.[2]

The charge density and DOS results can be used to obtain a crude approximation to the NMR Knight shift of the material. A simple development for the paramagnetic susceptibility of conduction electrons shows that the total magnetization is given by

$$M = \mu_B(N_+ - N_-) \quad \text{or} \quad M = \mu_B^2 D(E_F) B,$$

where N_+ is the concentration of spin up electrons, N_- is the concentration of spin down electrons, B is the applied field, and $D(E_F)$ is the density of states at the Fermi energy. This gives the paramagnetic spin susceptibility as $\chi_p^s = \mu_B^2 D(E_F)$.

If we consider the conduction electrons to be essentially free, we can add a diamagnetic contribution equal to $-\frac{1}{3}$ of the paramagnetic term to the total spin susceptibility.[19] We thus arrive at

$$\chi_{\text{total}}^s \approx \tfrac{2}{3}\mu_B^2 D(E_F). \tag{6}$$

In the absence of orbital and core-polarization contributions, the Knight shift is given by:

$$K = \Delta H/H = (8\pi/3)\langle |u_k(0)|^2\rangle_{E_F} \chi_{\text{total}}^s, \tag{7}$$

where $\langle |u_k(0)|^2\rangle_{E_F}$ is the average probability density at the resonant nucleus of all electronic states on the Fermi surface.

The product $\langle |u_k(0)|^2\rangle D(E_F)$ appearing in Eq. (7) can be estimated from the partial density of states, as $|\psi_s(0)|^2 D_s(E_F)$ where s denotes the atomic-valence s electron—2s for Li and 3s for Al, and $\psi_s(0)$ is the free-atom orbital evaluated at the nucleus.[20] This approach yields values of K_{Li} and K_{Al} which are essentially zero, within the accuracy of the present model. K_{Li} is very small because of the $2s - 2p$ intra-atomic charge transfer, with an additional ~0.25 electron charge transfer to

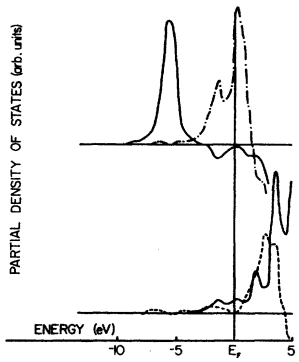

FIG. 6. Partial densities of states for Li $2s, 2p$ and Al $3s, 3p$ character in Li_5Al_4 cluster. Top: Al $3s$ (solid line), Al $3p$ (broken line); bottom: Li $2s$ (dashed line), Li $2p$ (solid line).

aluminum. K_{Al} is small because of the bonding shift of Al $3s$ character to a position well below E_F (see Fig. 5).

D. x-Ray emission

Soft x-ray emission band shapes are strongly dependent upon oscillator strength selection rules for transitions into the core hole state. The combination of parity selection and overlap factors for core states on A sites versus conduction-band orbitals on A or B sites can be exploited to provide essentially complete information on occupied conduction band composition.

In Fig. 6 we have shown partial densities of states D^{ν}_{nl} for lithium and aluminum valence orbitals (for the Li_5Al_4 cluster) in the vicinity of E_F. The results are qualitatively similar for the Al-centered cluster. Now the Li K emission spectrum consists of dipole-allowed Li $2p \rightarrow 1s$ and Al $3s, 3p \rightarrow$ Li $1s$ transitions, the latter (due to two-center overlap effects) being of reduced intensity. Our results suggest a rather weak emission band ~3 eV wide, followed by a well-defined low energy Al $3s$ satellite at ~6 eV below the Fermi edge. Al K emission should display a strong peak at E_F, a band width of ~3 eV, and essentially no cross-over satellites because of the depopulation of the Li $2s$ orbital. Al $L_{II,III}$ features will be dominated by transitions from Al $3s$, with weak structure extending to E_F due to a small amount of sp hybridization and mixing with Li basis states.

E. Vacancy cluster

The lithium-vacancy cluster $(V_{Li}Li_4Al_4)$ was treated in a manner analogous to that described for the A_5B_4 clusters. A single s-basis function (obtained as a potential well eigenstate) was placed in the center of the cluster to allow for the possibility of a bound state in the vacancy site, and to provide variational freedom to describe the conduction

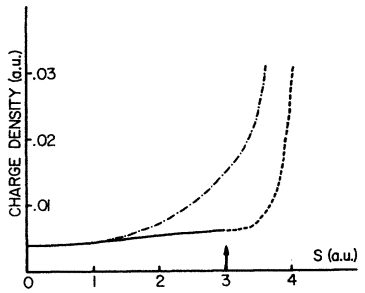

FIG. 7. Charge density for $(V_{Li}Li_4Al_4)$ lithium-vacancy cluster plotted along symmetry directions: [100], solid line; [111], dashed line; and $[\bar{1}\bar{1}\bar{1}]$, broken line.

electron tails in this region. The self-consistent MO solutions for this cluster show that the vacancy-localized state lies about 5 eV above the Fermi energy, with additional small amounts of the vacancy orbital mixed into occupied levels. The resulting charge distribution about the vacancy site is plotted in Fig. 7; ρ is seen to be rather spherical out to a distance of ~2 a.u. where the difference between Li and Al neighbor sites begins to be sizeable.

For positron states localized at vacancy sites, we may expect that the local bonding charge anisotropy will have important consequences for the annihilation γ-ray angular distribution.[21,22] The two-photon decay rate is governed by the overlap amplitude

$$A(\vec{p}) = \sum_n f_n \int d^3r\, e^{i\vec{p}\cdot\vec{r}} \varphi^*(\vec{r})\psi_n(\vec{r}) \qquad (8)$$

between the positron wavefunction φ and the occupied electron states, and we thus expect strong enhancements along the [111] and $[\bar{1}\bar{1}\bar{1}]$ directions. Comparison of experimental angular anisotropies with theory provides severe tests of vacancy structure models which cannot be obtained from lifetime data alone. From the theoretical side, one must learn to predict the relative contributions of core, conduction, and vacancy-trapped annihilation processes, and to assess the accuracy of positron wavefunctions. From the experimental side, one must obtain absolute precision of $\lesssim 1\%$ with reasonable angular resolution, using single-crystal specimens. To our knowledge, such data have not yet been obtained for alloy systems, but are available for a number of pure metals.[22] Experimental studies on the available single-crystal LiAl specimens would thus be quite interesting.

ACKNOWLEDGMENTS

We acknowledge helpful conversations with A. C. Switendick and A. Zunger concerning the band structure of LiAl, and thank Professor J. O. Brittain for discussions of experimental data.

†Research supported by the NSF.

*Permanent address: Department of Radiology, University of Illinois at the Medical Center, Chicago, Illinois 60612.

[1]E. Zintl and G. Brauer, Z. Phys. Chem. B 20, 245 (1933).

[2]H. E. Schone and W. D. Knight, Acta. Met. 11, 179 (1963).

[3]L. H. Bennett, Phys. Rev. 150, 418 (1966).

[4]J. R. Willhite, N. Karenezos, P. Cristea, and J. O. Brittain, J. Phys. Chem. Solids 37, 1073 (1976).

[5]Y. L. Yao, Trans. Met. Soc. AIME 230, 1725 (1964).

[6]P. Cristea, J. R. Willhite, J. O. Brittain, and C. R. Kannewurf (private communication).

[7]A. C. Switendick (private communication).

[8]J. C. Slater, *The Self-Consistent Field for Molecules and Solids* (McGraw-Hill, New York, 1974).

[9]K. H. Johnson, in *Advances in Quantum Chemistry*, edited by P.-O. Löwdin (Academic, New York, 1972), Vol. 6, p. 1.

[10]E. J. Baerends, D. E. Ellis, and P. Ros, Chem. Phys. 2, 41 (1973).

[11]A. Rosén, D. E. Ellis, H. Adachi, and F. W. Averill, J. Chem. Phys. 65, 3629 (1976).

[12]K. H. Johnson, R. P. Messmer, and J. W. D. Connolly, Chem. Phys. 11, 319 (1975).

[13]V. A. Gubanov and J. W. D. Connolly, Chem. Phys. Lett. 44, 139 (1976).

[14]M. Gupta, V. A. Gubanov, and D. E. Ellis, J. Phys. Chem. Solids 38, 499 (1977) and references therein.

[15]R. S. Mulliken, J. Chem. Phys. 23, 1833 (1955); J. Chem. Phys. 23, 1841 (1955).

[16]W. A. Harrison, *Solid State Theory* (McGraw-Hill, New York, 1970).

[17]W. Y. Ching, Ph.D. thesis, (Louisiana State University, 1974) (unpublished); W. Y. Ching and J. Callaway, Phys. Rev. B 9, 5115 (1974).

[18]R. P. Messmer, C. W. Tucker, Jr., and K. H. Johnson, Chem. Phys. Lett. 36, 423 (1975); R. P. Messmer, S. K. Knudson, K. H. Johnson, J. B. Diamond, and C. Y. Yang, Phys. Rev. B 13, 1396 (1976); T. Tanabe, H. Adachi, and S. Imoto, Japan J. Appl. Phys. 16, 375 (1977).

[19]For a critical discussion and comparisons with experiment, see e.g., W. D. Knight, Solid State Phys. 2, 93 (1956); P. Jena, T. P. Das, and S. D. Mahanti, Phys. Rev. B 1, 432 (1970).

[20]Slightly more quantitative results could be obtained by renormalization of free-atom wave functions to the Wigner-Seitz sphere. However, hybridization effects are of a similar magnitude, so that a direct averaging of MO states or energy band densities, as in Eq. (7), is probably required for reliable numerical estimates.

[21]R. N. West, Adv. Phys. 22, 263 (1973).

[22]*Positron Annihilation*, edited by A. T. Stewart and L. O. Roellig (Academic, New York, 1967). Data for $Li_{1-x}Mg_x$ alloys have been interpreted qualitatively in terms of the rigid-band model; *ibid.*, p. 38; and A. T. Stewart, Phys. Rev. 133, A1651 (1964).